On-Orbit, Non-destructive Surface Surveillance and Inspection with Convolution Neural Network

Sanjay Lakshminarayana[1(✉)], Shubham Bhaskar Thakare[2], and Krishna Vamshi Duddukuru[1]

[1] Department of Civil and Industrial Engineering - Aerospace Engineering Division, University of Pisa, 56126 Pisa, Tuscany, Italy
sanjaylakshminarayana@outlook.com
[2] Department of Mechanical Engineering, Wichita State University, Wichita, KS 67260, USA
sxthakare@wichitastate.edu

Abstract. In this paper, the concept for on-orbit, non-destructive Infrared survey and inspection of the surface defects on an inter-planetary human module with large surface area and power capabilities, for long flight duration is derived. Automated Probe with thermal imaging camera is used to capture 2D thermal images at that position during rendezvous around the human module. Thermal imaging datasets are classified under binary classification problem and Custom CNN with TensorFlow Architecture is developed. The test accuracy obtained at initial stage of development is about 92%. Converted 2D high resolution grey thermal images are segmented to measure cracks by mapping the pixels. Upon identification of fault position, on-board crew is alerted and original designer is updated, to address the problem remotely. Thereby, an effort has been done herein to significantly reduce the crew EVA spent in survey for surface faults during mission in harsh space environment and the corresponding pre-mission training requirements.

Keywords: Extra vehicular activity · Thermal imaging · Convolution neural network - tensorflow · On orbit servicing and maintenance · Non-destructive testing · Image segmentation

1 Introduction

With the public interest, private investments in human exploration mission to moon and mars rising, the development of new techniques and artificial intelligence enabled machines suitable for manufacturing and servicing will play key role in meeting critical requirements for long term human missions. Especially for settlement missions and cargo transportation to moon, mars and beyond. Private space companies like SpaceX, Virgin galactic etc. aim to build alternate settlements and increase the access to space at public level.

S. Joshi et al. (Eds.): SpacSec 2021, CCIS 1599, pp. 283–293, 2022.
https://doi.org/10.1007/978-3-031-15784-4_22

As defined in Sarafin (1995), fatigue damage is gradual degradation of material under cyclic loading conditions, causing small cracks to form in the vicinity of microscopic defect areas. European Cooperation for Space Standardization (ECSS) (2009a, 2021) underlines standard procedure for choosing the type of Non-destructive testing (NDT), based on the initial crack size, depth and shape factors. Standard tests are allocated for highest probability of crack detection and for fracture control is advised. But structural elements have defects located in worst possible areas and orientations. NDT method used to test for the defects before launching may not be successful at detecting every crack due to an upper bound on the properties of the geometry. It is also known that, Dynamic loads which vary the fracture toughness of the geometry under the action of sufficient number of cycles of amplitude tend to propagate cracks even in most adequate of environments. [1–4] If the detected cracks are within the limits for the structural design of a particular mission, it is a well-known fact that inter-planetary space travel is posed by several threats. By travelling at high speeds, the impacts of the micro meteors can initiate or lead to propagation of defects, increasing the probability of permanent damage. Shielding developed currently is suitable for small-scaled satellites, up-scaled version is expensive and impractical.

For human missions, it will be advantageous from the safety and relaunch cost point of view, to carry on board equipment that is capable of custom delivery of solutions, particularly concerning leak response. These operations not only require a specially trained crew, but also tedious procedures and require long duration training on ground before ability to perform EVA. Also, defect areas are mostly posed with additional challenge and difficulty to access with life threat to the crew. Even with tedious and expensive procedure, the effectiveness of the solution is nowhere near expected efficiency. Also, owing to lack of complete awareness of the system being repaired due to the limited human capacity, knowledge gaps between the original ground designer and the trained crew exist.

With the limited information which exists on the real time On-Orbit Upgrade and repair activities, existing models are based on the most notable repair in space history, viz, Hubble space telescope. During Hubble space program activities, astronauts received tens of months of constant training and practice at specially designed training facilities, to perform replacement and repairs to the space telescope. EVA to fix Hubble, took a handful of days with 8-hour long shifts performed by Astronauts. Exploring the possibilities of developing a model for application in real time, Hastings et.al applied Monte Carlo simulation to randomize variables for servicing scenarios to map the time and its impact on satellites reliability. Results clearly indicates that servicing albeit with a small percentage of risk is beneficial for life extension of satellite. Working proof of reliable operation due to inspection and servicing is Hubble telescope itself. However, activities performed during Hubble servicing are not completely relevant to the current day scenario, especially for human missions. In future, a deeper and more generalized architecture is required for human missions, especially of inter-planetary nature [5]. Fatigue damage is inevitable during long term mis-

sions with corresponding large surface area of the structures of various modules. It can be prevented with real time inspection for damage and to overcome the limitation of some of the standardized ground-based tests. By developing alternative solutions, without the requirement of highly skilled operator or EVA's.

The architecture proposed involves an automated probe that performs inspection of surface, directly exposed in space, without direct physical contact between the instrument and the test surface area. Infrared (IR) thermography is non-destructive testing technique which works by measuring the temperature at each point on the surface. The surface temperature is recorded and analysed with an IR Camera. The thermal camera displays the surface temperature in form of an image [6]. Using Thermal diffusion theory, the temperature profiles in and around the cracks with finite depth has already been modelled. In the image captured by the thermal camera, differences in surface temperature are observed as image gradients. The data provides an advantage over other methods with high detection probability with distinct information about defects. As applied in Yang et.al, thermal excitation provided by external source on to the surface, enables better detection of real cracks when thermal source and crack are along same direction, resulting in higher temperature gradients due to enhanced heating effect. Further, temperature profiles of deep surface cracks and shallow surface scratch has been modelled. Crack is classified for a steel plate, based entirely on surface temperature gradients formed on either side of the vicinity of crack. Results clearly indicate that Temperature gradients assist to identify the defect, as the temperature variation is high in its vicinity [4,7].

The surface defect detection in thermal image is made possible by computer vision algorithms. Working similar to human vision, are fast, accurate in identifying and classifying the object data. Faster Region-CNN, based on Regional Proposal Network (RPN) detects cracks in an effective way compared to Region-CNN, similar architecture is employed in Yang et.al, Zemmar et al., for-crack detection and analysis in steel plate and biological materials in 3D respectively. These require relatively large computing infrastructure and real-time classification of object data is difficult. You only Look Once (YOLO) architecture is extremely fast at processing multi-resolution data in real-time, outperforming R-CNN and Mobile Single Deep Neural Network (SDN) in terms of Average Precision and Detection time by a margin. YOLO algorithm is based on regression methods, considers the whole image and calculates the class probability to label the bounding boxes. Alternately, in Zhai et.al unmanned aerial vehicle (UAV) systems are being utilized for surveillance and inspection purposes during flight. CNN based on RESNET architecture employing multi-task binary classification problem has been developed. Model can detect, process and classify spatial image data in real time, with variety of defects over multiple image backgrounds. UAV can achieve fully automated surveillance, data acquisition, diagnostics and situational understanding. The architecture can easily be adopted for other applications. As discussed, YOLO is faster but CNNs adopting PythonTensor-Flow which is symbolic math library based on data-flow and differentiable programming allow for far more in-depth customisation especially for image classification

applications, [7–13]. Also, during space travel, defect of every type is relevant and potentially life threatening to on-board crew. Therefore, Tensor-Flow based CNN architecture is adopted in this paper for deeper customization of Real-time image datasets at relatively lower computing cost.

2 Design of Operation

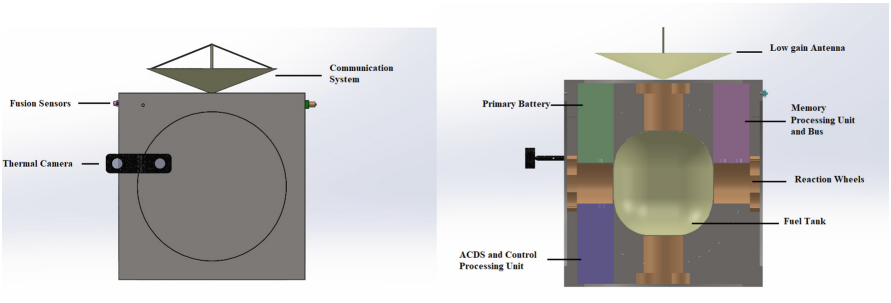

Fig. 1. 3D CAD representation of the probe

The CAD model shown in Fig. 1 represents the Probe with IR thermal imaging, which consists of emitter and receiver. Working in real time, sensors are fixed on all faces. It is used to achieve ease of operation in complex spaces. The mass of the main sub-systems included in the probe are discussed in Table 1. Even though, it is beyond scope of this paper to investigate Complete Automation of probe in terms of Navigation and Guidance, Propulsion, detailed Power budget, Communication and the operation of the instruments, Surveillance procedure assumes conditions below. During operation,

(a) Relative motion between the probe and the human module is assumed to be non-uniform. Automated probe is expected to rendezvous around the human space module at nearly constant distance to the surface assisted by imparting control force powered by an on-board propulsion system with Fusion sensors for attitude guidance. Additionally, ACDS is equipped with 6 - Reaction wheels along 3 Axes with accuracy of 4 RPM, operating at 0.2 W, on-board propulsion system is used for momentum dumping when necessary. It is required to limit variations that arise from perturbations in attitude and distance during operation of thermograph, to obtain high resolution images (without blur).
(b) To counter external noise, assuming that peak intensity of external radiation is along normal to the surface area being inspected. Probe is required to operate parallel to the surface plane of human module to block the noise.

(c) Assuming the outer surface of the human module is in thermal equilibrium with surroundings. Probe is required to incident energy on to the surface of the module, by the means of Light Source for thermal excitation to induce significant temperature difference (against background noise). The large temperature gradient improves, temperature resolution in the image data recorded by thermograph. Thermal camera operates at voltage input of 16V DC, in wavelength range of 1–14 microns with a minimum detector array size of 144 × 144 and Operating at temperature range of [50,120] K.

Table 1. Mass budget as represented in Fig. 1b

System	Component/Function	Wt in Kg
Fusion Sensors and Processing Units	Proximity sensor	0.1
	Inertia sensor	0.2
	IR sensor	0.1
	Reaction wheels	0.75
	Storage, CPU and BUS	7.5
Fuel	Control Force	35
Communication	Ground/Module/Probe	15
IR Thermography	Thermal Imaging Camera	4
	Processing Tools & Memory	4
Emitter and Receivers		2.8
Misc.		1
Total Mass Budget		70

3 Auto - Identification of Defects

The development of artificial neural network which enables to classify the thermal images with defect from the thermal image without defect, by well-known binary classification problem with Python - Tensor-Flow is presented in Sect. 3.1 and Sect. 3.2. Results are discussed in Sect. 4.

3.1 Preparing Image Data-set

There is no suitable pre-existing data-set available for this study nor a pre-trained CNN based on the presented architecture. The data obtained, consists of multiple types of defects at various developing stages as shown in Fig. 2. Private firms successfully implemented, IR Thermography to identify during early stage of defects, Cracks, Live Gas Leaks in piping as shown in Fig. 2(b), short circuits in Solar Arrays etc. Figure 2(b) represents, Spots with abnormal temperature distribution caused by Live Leakage, Cracks and Fractures at surface and sub-surface in Piping. In Fig. 2(a), 2(c) and 2(d), hot spots identify defective cell,

short circuit, defect at connection points of solar panel. The idea is to collect images relevant to Space applications, Test sample of 68 was obtained from [14–21] with variety of resolution, out of which 32 samples were positive for defect. Sample size is increased with data augmentation, it is necessary to avoid over-fitting and it resulted in increasing the test accuracy result of the base-model.

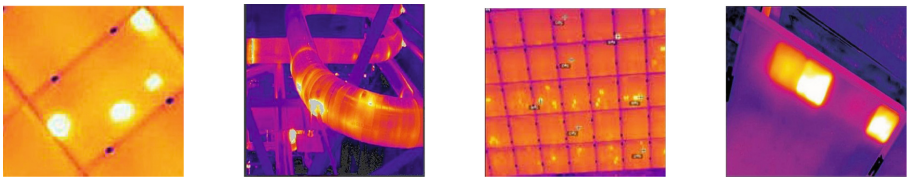

Fig. 2. Thermal image dataset with defects

Each image is stored as Data Frame. Image with and without defects are concatenated along same axis, data frames are split further with train Test flip function [22–24]. Dataset comprised of images, with size 502 × 317. Greater than 75% of the data frame is used to train and remaining as test set with Image pixel class as binary. Because, obtained datasets were of varying size and resolution, to augment the datasets without loss of resolution, the images were sliced to 250 × 250. Standard Encoding of the thermal images are done in RGB scale. The classified Data frame is composed of 330 trained set, 338 test set images and 82 validated set.

3.2 Network Architecture and Implementation

The problem is considered as binary classification problem where in likelihood of the data belonging to either (a) With Defect assigned integer value 1 or (b) Without Defect assigned integer value 0 is predicted. A standard TensorFlow CNN implemented in [25] but of 4 layers with Max pooling with size[2 × 2], 3 fully connected layers is considered given the size of the available dataset. The input image is of dimensions (250, 250, 3), with max pool layer of stride (2, 2). The first layer is comprised of 32 Filters, rest of the 3 layers are of 64 filters. At 2nd Layer, input dimension is reduced to (121, 121, 64) and (58, 58, 64), (27, 27, 64) for 3rd and 4th layers respectively. The output of the fully connected 4th layer is passed on to SoftMax layer to normalize the classification vector. All the hidden layers use ReLu activation function, as it is very well known to decrease the likelihood of vanishing gradient problem and in this case, also for faster learning. The designed CNN is represented in Fig. 3.

3.3 Training Experiments

The training corresponds to varying three parameters, Image dataset size (D), Number of Nodes (N) and Learning Rate (I), with I = [0.001, 1], D = [25, 100]

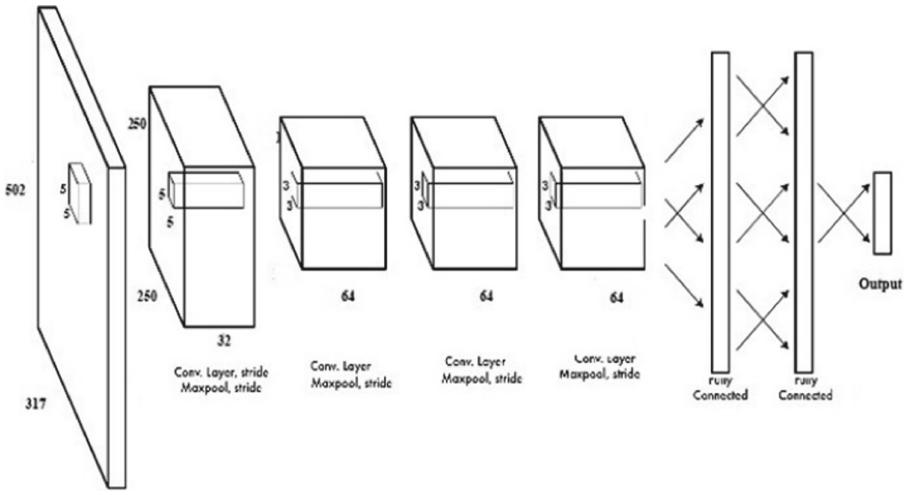

Fig. 3. 4-Layer CNN model

%, N = [16, 32, 64, 128, 256]. For each experiment, the value of accuracy for every Epoch = [100] was recorded, to identify the best model. Also, training was performed on Python IDE on a Personal Computer with 16 GB memory.

3.4 Image Segmentation

Thermal Image with Defect Fig. 4(a) is then converted from Standard RGB to grey scale, during which the quality of the image is not affected. Grey images limit the need of large storage space, the environment in which, the images captured favour their use as saturation if present, in the original image is reduced upon conversion. Also, Gray images preserve Temperature gradients of the original thermal image, In terms of proportionate gradients in gray scale. Therefore, Defect information is not lost, entirely. Gray Image is shown in Fig. 4(b). Before measuring the crack, image is enhanced by contrast stretching [9,26–28] as shown in Fig. 4(b). Image is segmented by setting an arbitrary threshold value as the defined value and the image with segmented crack is obtained as shown in Fig. 4(c). Clearly, the Crack Width (L_C) is the ratio of the product of calibration length (C_L) and crack pixels (P_L) to the calibration pixels (C_P) as given by Eq. (1).

$$L_C = P_L * C_L / C_P \tag{1}$$

4 Result Discussion

The best value of accuracy was obtained for I = [0.001], N = [64], Epoch = 100 with D = 98% yields an accuracy of 92% with corresponding f1 score

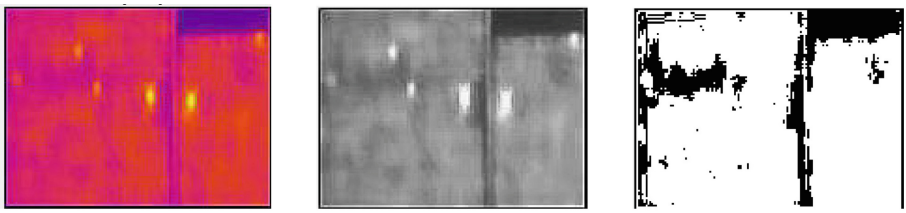

Fig. 4. (a) High resolution thermal image identified for defect (b) Thermal image converted to gray scale (c) Segmented with multiple defects (Color figure online)

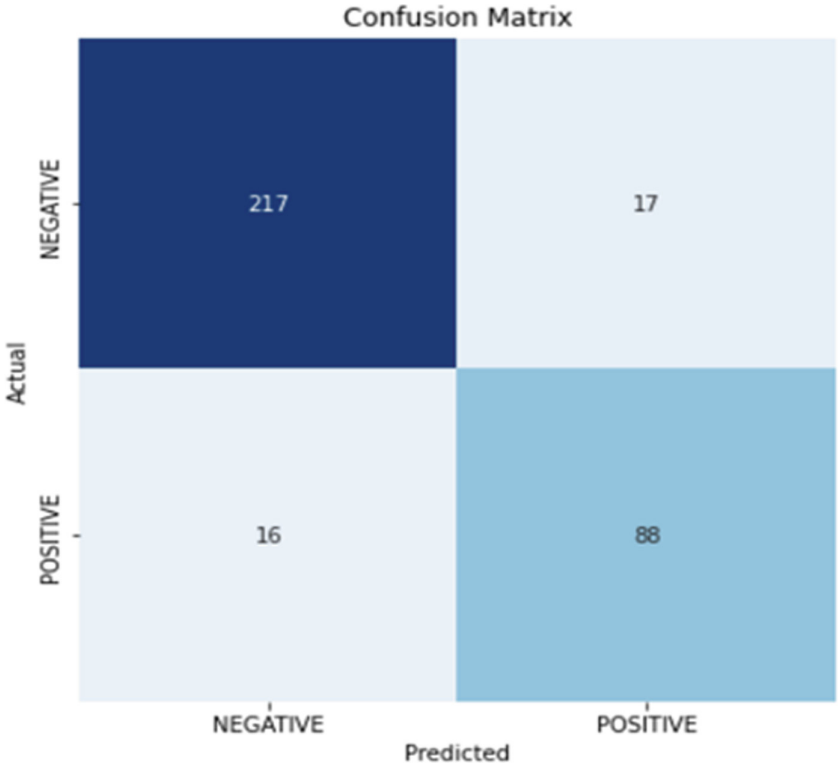

Fig. 5. Confusion matrix of CNN

obtained from Fig. 5 is 92%. Clearly the accuracy is dependent on the training image dataset and resolution of the image in the data set. By obtaining, real data from space missions, the accuracy value for CNN architecture proposed in this paper, can surpass 95% easily. It is important to bear in mind that in this paper, the prime focus is to investigate and provide a proof of concept for an automated probe based on CNN in rendezvous around human module. Equipped

with thermal camera, along with Fusion sensors. A probe, capable of surveying the surface area for defects, identified by processing the thermal image data as shown in Sect. 3.1 to Sect. 3.3. Upon identification of defect, the image with defect is processed with procedure in Sect. 3.4 and On-board crew is alerted by the probe for further examination.

In Sect. 3.4, Using equation (1), the image size in Fig. 4 is arbitrarily taken to 154×176 (width $\times$ height) pixels, by taking 1 pixel = 1/100th of an Inch as reference. The Height (almost equal to the original height of the object in Fig. 4) of the major crack is maximum 14.08-inch. Also, by trial and error, threshold value for this model is best between 0.45 and 0.55.

5 Conclusion

Concept for a working On Orbit, IR- Non-Destructive for Real-time Survey and Inspection of surface defects adopting custom developed CNN has been investigated. Probe represented in Sect. 2 with completely automated sub-systems holds potential to enable better access to majority of the module surface. Fully Automated Probe configuration can be used commonly for surveillance, independently of module design and Area Spans. Probe, at about the size of micro-satellite can be launched, attached with other modules in single launch. However, operation is at cost of on-board propulsion system utilized for translation motion around module, on-board batteries charge-discharge cycle, limiting the surveillance time.

Method in Sect. 3.1, 3.2 and 3.3 provide greater adaptability and automation for survey and inspection. Section 3.4 revisits known image segmentation technique in measuring the dimension of the defect and thereby its extent. The design assists with Extra Vehicular Activity, eliminates exposure to life threatening situation for crew and results in reduction of launch and operation costs. Such operations primarily require many months of training and preparation on Earth, including tens of hours of spacewalks for detection and fixing of defects on large surface spans. The mass of the probe is kept below 100 Kg and the total wattage about 100 W. The proposed CNN model accuracy rate at defect identification and classification is best at 92%. But with real-time mission data, it is expected to reach 95% and higher. Further, Post-Processed Data can be manually implemented with CAD software tools to regenerate the 3D data and to design replacements for the defect areas by the original designer. Finally, 3D printing solutions available on-board will enable crew to implement the new design to resolve or replace the defect area, which is the only manual task requiring EVA.

Acknowledgement. We express special thanks to Dr Vinod Singh Yadav, Assistant Professor, National Institute of Technology, Uttarakhand, India. Dr Amit Kumar Bairwa, Manipal University Jaipur and Dr RoopaShree Tantri for their valuable guidance and motivation in completion of the work.

References

1. Sarafin, T.P., Larson, W.J.: Spacecraft Structures and Mechanisms-from Concept to Launch. Microcosm, Torrance (1995)
2. European Cooperation for Space Standardization (ECSS). https://ecss.nl/item/?glossary_id=1776. Accessed 6 Mar 2021
3. European Cooperation for Space Standardization (ECSS) Non-destructive testing. https://ecss.nl/standard/ecss-q-st-70-15c-non-destructive-testing/. Accessed 1 May 2021
4. Rodríguez-Martín, M., Lagüela, S., González-Aguilera, D., Martinez, J.: Prediction of depth model for cracks in steel using infrared thermography. Infrared Phys. Technol. **71**, 492–500 (2015). https://doi.org/10.1016/j.infrared.2015.06.013
5. Hastings, D.E., Joppin, C.: On-orbit upgrade and repair: the Hubble space telescope example. J. Spacecr. Rockets **43**, 614–625 (2006). https://doi.org/10.2514/1.15496
6. Speakman, J.R., Ward, S.: Infrared thermal imaging: principles and applications. Zoology-Jena- **101**, 224–232 (1998)
7. Yang, J., Wang, W., Lin, G., Li, Q., Sun, Y., & Sun, Y.: Infrared thermal imaging-based crack detection using deep learning. IEEE Access **7**, 182060–182077 (2019). https://doi.org/10.1109/access.2019.2958264
8. Zemmar, A., Lozano, A.M., Nelson, B.J.: The rise of robots in surgical environments during COVID-19. Nat. Mach. Intell. **2**, 566–572 (2020). https://doi.org/10.1038/s42256-020-00238-2
9. Santhi, B., Krishnamurthy, G., Siddharth, S., Ramakrishnan, P.K.: Automatic detection of cracks in pavements using edge detection operator. J. Theor. Appl. Inf. Technol. **36**(2), 199–205 (2012)
10. Barreira, E., de Freitas, V.P.: Evaluation of building materials using infrared thermography. Construct. Build. Mater. **21**(1), 218–224 (2007)
11. Redmon, J., Divvala, S., Girshick, R., Farhadi, A.: You only look once: unified, real-time object detection. In: 2016 IEEE Conference on Computer Vision and Pattern Recognition (CVPR). Presented at the 2016 IEEE Conference on Computer Vision and Pattern Recognition (CVPR). IEEE (2016) https://doi.org/10.1109/cvpr.2016.91
12. Li, Y., Han, Z., Xu, H., Liu, L., Li, X., Zhang, K.: YOLOv3-Lite: a lightweight crack detection network for aircraft structure based on depthwise separable convolutions. Appl. Sci. **9**, 3781 (2019). https://doi.org/10.3390/app9183781
13. Zhai, X., Liu, K., Nash, W., Castineira, D.: Smart autopilot drone system for surface surveillance and anomaly detection via customizable deep neural network. In: International Petroleum Technology Conference. OnePetro (2020). https://doi.org/10.2523/IPTC-20111-MS
14. http://tmt.co.il/product/solar-panels-thermal-visual-inspection/ . Accessed 17 Oct 2021
15. https://westerninfrared.com/problems/solar-panels/ . Accessed 17 Oct 2021
16. López-Fernández, L., Lagüela, S., Fernández, J., González-Aguilera, D.: Automatic evaluation of photovoltaic power stations from high-density RGB-T 3D point clouds. Remote Sens. **9**(6), 631 (2017). https://doi.org/10.3390/rs9060631
17. PhotoVoltaic Solutions https://kitawa.de/en/thermography-pv-systems. Accessed 17 Oct 2021
18. Thermography. https://www.murcal.com/, https://www.murcal.com/pdf20folder/15.testo_thermography_guide.pdf. Accessed 17 Oct 2021

19. Balasubramani, G., Thangavelu, V., Chinnusamy, M., Subramaniam, U., Padmanaban, S., Mihet-Popa, L.: Infrared thermography based defects testing of solar photovoltaic panel with fuzzy rule-based evaluation. Energies **13**(6), 1343 (2020). https://doi.org/10.3390/en13061343
20. Runnemalm, A. and P. Broberg.: Surface crack detection using infrared thermography and ultraviolet excitation. Quant. InfraRed Thermography, 1–7 (2014)
21. Lee, S.Y., Tama, B.A., Moon, S.J., Lee, S.: Steel surface defect diagnostics using deep convolutional neural network and class activation map. Appl. Sci. **9**(24), 5449 (2019). https://doi.org/10.3390/app9245449
22. Inoue, H.: Data augmentation by pairing samples for images classification. arXiv preprint arXiv:1801.02929 (2018)
23. Paper, D.: Scikit-learn classifier tuning from complex training sets. In: Hands-on Scikit-Learn for Machine Learning Applications, pp. 165–188. Apress, Berkeley (2020). https://doi.org/10.1007/978-1-4842-5373-1_6
24. Nelli, F.: pandas in depth: data manipulation. In: Python Data Analytics, pp. 131–165. Apress, Berkeley (2015). https://doi.org/10.1007/978-1-4842-0958-5_6
25. Han, Z., Chen, H., Liu, Y., Li, Y., Du, Y., Zhang, H.: Vision-based crack detection of asphalt pavement using deep convolutional neural network. Iran. J. Sci. Technol. Trans. Civ. Eng. **45**(3), 2047–2055 (2021). https://doi.org/10.1007/s40996-021-00668-x
26. Sternberg, S.R.: Grayscale morphology. Comput. Vision Graphics Image Process. **35**, 333–355 (1986). https://doi.org/10.1016/0734-189x(86)90004-6
27. Chen, X., Li, J., Huang, S., Cui, H., Liu, P., Sun, Q.: An automatic concrete crack-detection method fusing point clouds and images based on improved otsu's algorithm. Sensors **21**, 1581 (2021). https://doi.org/10.3390/s21051581
28. Li, S., Zhao, X.: Image-based concrete crack detection using convolutional neural network and exhaustive search technique. Adv. Civ. Eng. **2019**, 1–12 (2019). https://doi.org/10.1155/2019/6520620